

Article

Structure, Mechanical Properties and Friction Characteristics of the Al-Mg-Sc Alloy Modified by Friction Stir Processing with the Mo Powder Addition

Tatiana Kalashnikova ^{*} , Evgeny Knyazhev , Denis Gurianov , Andrey Chumaevskii, Andrey Vorontsov , Kirill Kalashnikov , Natalya Teryukalova and Evgeny Kolubaev

Institute of Strength Physics and Materials Science, Siberian Branch of the Russian Academy of Sciences, pr. Akademicheskii, 2/4, 634055 Tomsk, Russia; clothoid@ispms.tsc.ru (E.K.); gurianov@ispms.ru (D.G.); tch7av@ispms.ru (A.C.); vav@ispms.ru (A.V.); kkn@ispms.tsc.ru (K.K.); natali.t.v@ispms.ru (N.T.); eak@ispms.ru (E.K.)

* Correspondence: gelombang@ispms.tsc.ru

Abstract: In this study, samples of Al-Mg-Sc alloy were investigated after friction stir processing with the addition of Mo powder. Holes were drilled into 5 mm-thick aluminum alloy sheets into which Mo powder was added at percentages of 5, 10, and 15 wt%. The workpieces with different powder contents were then subjected to four passes of friction stir processing. Studies have shown that at least three tool passes are necessary and sufficient for a uniform Mo powder distribution in the stir zone, but the number of required passes is higher with an increase in the Mo content. Due to the temperature specifics of the processing, no intermetallic compounds are formed in the stir zone, and Mo is distributed as separate particles of different sizes. The average ultimate strength of the composite materials after four passes is approximately 387 MPa in the stir zone, and the relative elongation of the material changes from 15 to 24%. The dry sliding friction test showed that the friction coefficient of the material decreases with the addition of 5 wt% Mo, but with a further increase in Mo content, returns to the original material values.

Keywords: friction stir processing; aluminum alloys; tribology; microhardness; microstructure; mechanical properties; molybdenum



Citation: Kalashnikova, T.; Knyazhev, E.; Gurianov, D.; Chumaevskii, A.; Vorontsov, A.; Kalashnikov, K.; Teryukalova, N.; Kolubaev, E. Structure, Mechanical Properties and Friction Characteristics of the Al-Mg-Sc Alloy Modified by Friction Stir Processing with the Mo Powder Addition. *Metals* **2022**, *12*, 1015. <https://doi.org/10.3390/met12061015>

Academic Editors: Guoqing Gou, Qing Zhang and Gongwen Gan

Received: 1 June 2022
Accepted: 14 June 2022
Published: 15 June 2022

Publisher's Note: MDPI stays neutral with regard to jurisdictional claims in published maps and institutional affiliations.



Copyright: © 2022 by the authors. Licensee MDPI, Basel, Switzerland. This article is an open access article distributed under the terms and conditions of the Creative Commons Attribution (CC BY) license (<https://creativecommons.org/licenses/by/4.0/>).

1. Introduction

Friction stir processing (FSP) is a relatively simple and cost-effective method for the local hardening of a metal product. It is suitable for a wide range of materials and results in grain structure refinement and the elimination of internal defects such as pores and discontinuities, all of which have a positive effect on the product's properties. For example, the FSP of additive materials with large dendritic grains increases the ultimate tensile strength and other physical-mechanical properties [1–3]. Additionally, the process itself represents the plasticized material flow movement (i.e., material stirring), and this makes it possible to add to the stir zone the material needed (metals, ceramics, or carbon-based substances) in the form of powder, wires, or plates for the production of composite materials.

Aluminum alloys are a valuable structural material due to their light weight, strength, and corrosion resistance [4]. Improving the performance characteristics of aluminum alloys leads to a weight saving of final structures and products, which in turn reduces energy costs. The development of new aluminum-based alloys and composites can broaden the areas of their application. For example, the rubbing parts are mainly made of copper alloys or steels, and replacing them with aluminum alloys will lead to a significant weight saving of approximately 2–3-fold in these components. Studies of Al₂O₃ particle-reinforced aluminum alloy 6061 showed a significant reduction in wear compared to the original alloy [5]. The use of silicon carbide as one of the components of the aluminum-matrix composite also increases the wear resistance of the product [6].

The development of new ways to harden and improve the wear resistance of aluminum alloys is ongoing to this day, including various methods such as wire-based electron beam additive manufacturing with an addition of molybdenum powder [7].

Nowadays, the production of aluminum-based composite materials by the FSP method is considered by many scientists. The powders of nitrides [8], oxides [9,10], pure metals [11–14], carbides [15–18], and high-entropy alloys [19] can be used as modifying additives. The addition of powders is considered not only in the case of friction stir processing but also in welding. This contributes to producing more durable welded joints [20].

The creation of composites with molybdenum aluminides attracts researchers more and more due to their combination of high mechanical properties and heat resistance. Studies show that the use of Mo additives as an alloying component of aluminum alloys leads to a significant increase in microhardness values due to the formation of intermetallic particles such as $Al_{12}Mo$ and Al_5Mo [21,22].

Thus, the aforementioned prospects for the development of new composite materials causes the relevance of this work, specifically the study of aluminum-matrix composite production with different Mo powder content by the friction stir processing method.

2. Materials and Methods

In this work, workpieces—5 mm-thick rolled sheets of Al-Mg-Sc alloy—were selected as samples for this study. The chemical composition of the alloy is shown in Table 1. Holes were drilled in the workpieces on a milling machine with an increment of approximately 5 ± 0.05 mm, a depth of 3 mm, and a diameter of 1.5, 2.0, and 2.5 mm for 5, 10, and 15 wt% of Mo content, respectively. FSP was carried out on an experimental machine at the Institute of Strength Physics and Materials Science SB RAS (ISPMS SB RAS, Tomsk, Russia). A tool with a pin height of 3 mm, a pin base diameter of 8 mm, a pin end diameter of 6 mm, and a shoulder width of 16 mm was chosen to perform the processing. The number of passes was chosen from 1 to 4 for all workpieces. The FSP parameters are shown in Table 2. The FSP process scheme is shown in Figure 1. The tool loading force (P) was reduced to avoid excessive tool penetration into the workpiece during the first passes. Among other things, this is related to the specific features of the equipment used, where the tool position control is based on the loading force rather than the coordinate. The marking of the samples corresponds to the percentage of powder content and the number of passes, so for 5 wt%, the samples are marked as 5.1, 5.2, 5.3, and 5.4 for 1, 2, 3, and 4 passes, respectively. For 10 wt%, numbering is 10.1–10.4, and for 15 wt%—15.1–15.4.

Table 1. Chemical composition of Al-Mg-Sc alloy, wt%.

Al	Mg	Mn	Sc	Zr
Base	5.3–6.3	0.2–0.6	0.17–0.35	0.05–0.15

Table 2. Friction stir processing parameters for workpieces with 5, 10, 15 wt% Mo content.

No. of Pass	V (mm/min)	ω (rpm)	P (kg)		
			5 wt%	10 wt%	15 wt%
1	90	500	1080	950	860
2	90	500	1100	980	900
3	90	500	1150	1000	950
4	90	500	1150	1050	1000

Two-dimensional computer tomography was performed on a YXLON Cheetah EVO (YXLON International GmbH, Hamburg, Germany) to examine the material structure and detect defects. An Altami MET1-C optical microscope (Altami Ltd., Saint Petersburg, Russia) was used to evaluate the macro- and microstructure of the produced composites. The microstructure, phase, and elemental composition were studied using a JEM-2100 transmission electron microscope (JEOL Ltd., Akishima, Japan).

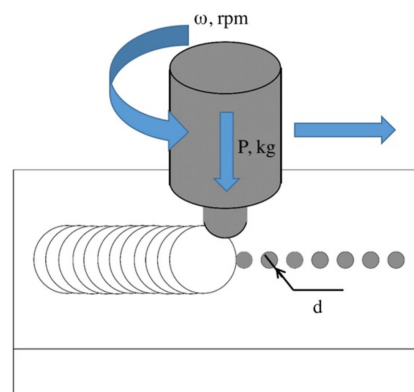


Figure 1. Scheme of the production of a composite based on an Al-Mg-Sc alloy with the addition of Mo powder via friction stir processing. ω —tool rotation speed; P —tool loading force; d —diameter of a hole for the powder addition.

The universal testing machine “UTS 110M-100” (TestSystems, Ivanovo, Russia) and microhardness tester Duramin 5 (Struers A/S, Ballerup, Denmark) were used for the assessment of the mechanical properties of samples. The TRIBOtechnic tribometer (Tribotechnic, Clichy, France) was used to measure the friction and wear characteristics of the samples. The dry sliding friction test was carried out according to the pin-disk scheme. Samples for friction tests were cut from the stir zone along the tool travel line with the shape of pins sized 3 mm × 3 mm × 10 mm. The load, rotation speed, and sliding path length were experimentally selected and were 12 N, 250 rpm, and 942 m, respectively.

3. Results

3.1. Stir Zone Macrostructure

The plates with 5% Mo powder content after the first processing pass showed a high non-uniformity of the structure (Figure 2 (5.1)). The structure is represented by “onion rings” with partially mixed molybdenum powder; however, most of the powder remained concentrated near the originally drilled holes, which led to the formation of voids.

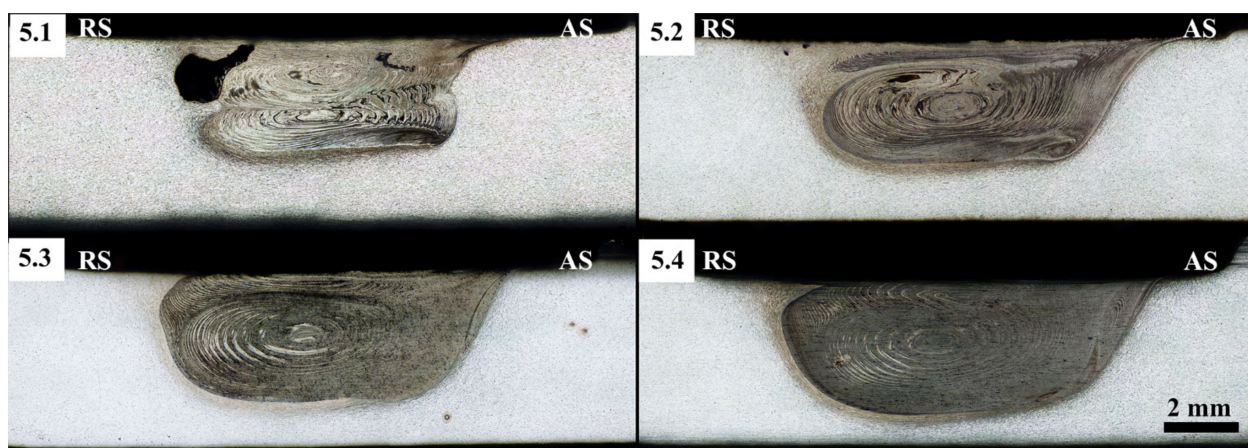


Figure 2. Al-Mg-Sc alloy macrostructure after FSP with 5 wt% Mo after 1–4 passes (samples 5.1–5.4). AS—advancing side, RS—retreating side.

After the second pass, the Mo powder is more uniformly distributed over the stir zone (SZ), and voids are practically not observed anymore. However, during the second pass, the powder additive is not completely distributed in the volume of the processed area, as evidenced by the computer tomography (CT) results (Figure 3 (5.2)). Subsequent passes lead to a more uniform distribution of the alloying component (Figure 3 (5.3,5.4)). As can be seen from the CT images, during the first pass, the tool captures powder layers on the

advancing side, but apparently, the powder adheres to the tool in large clusters as a result of adhesive interaction, resulting in a lack of material that could fill the void from the hole.

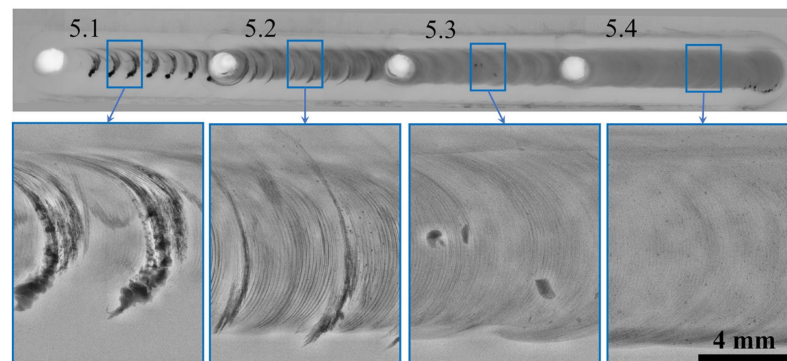


Figure 3. CT images of the processed area of Al-Mg-Sc alloy with 5 wt% Mo.

The nature of the stir zone formation at different stages is also worth noting. At the first pass, in sample 5.1 (Figure 2), the stir zone is formed by two flows, as a result of which two nuggets are observed: the first one is formed in the workpiece monolithic area, and the second one is formed in the area of the filled hole. In this case, the powder in the hole is predominantly transferred to the lower nugget, while the workpiece material filling the hole forms the upper nugget by upward flows. A similar character of SZ formation was observed in [21], but there it was caused by the large workpiece thickness and heterogeneity of temperature effects. Multiple processing eliminates the non-uniformity of the stir zone, resulting in a monolithic nugget and the zone of tool shoulder influence (Figure 2 (5.2–5.4)), and as stated earlier, with an increasing number of passes, the powder is more uniformly distributed in the entire SZ, which is confirmed by CT data.

When the alloying additive content is increased up to 10 wt%, the pattern of the stir zone formation during the first pass changes: a typical SZ with one nugget is formed instead of two, and the powder is distributed more uniformly than for 5 wt%, but is also mainly concentrated in the lower part of the SZ.

Although samples with high Mo content showed no large defects on optical images after the primary and subsequent processing (Figure 4), the first pass also forms defects such as voids, which can be seen from CT images (Figure 5). However, the second pass already considerably improves the structure by distributing large powder clusters. At the same time, the CT images show that due to the increase in the powder particle fraction, even on the first pass, the powder is stirred up almost the entire distance between the holes, due to which a more homogeneous SZ is formed.

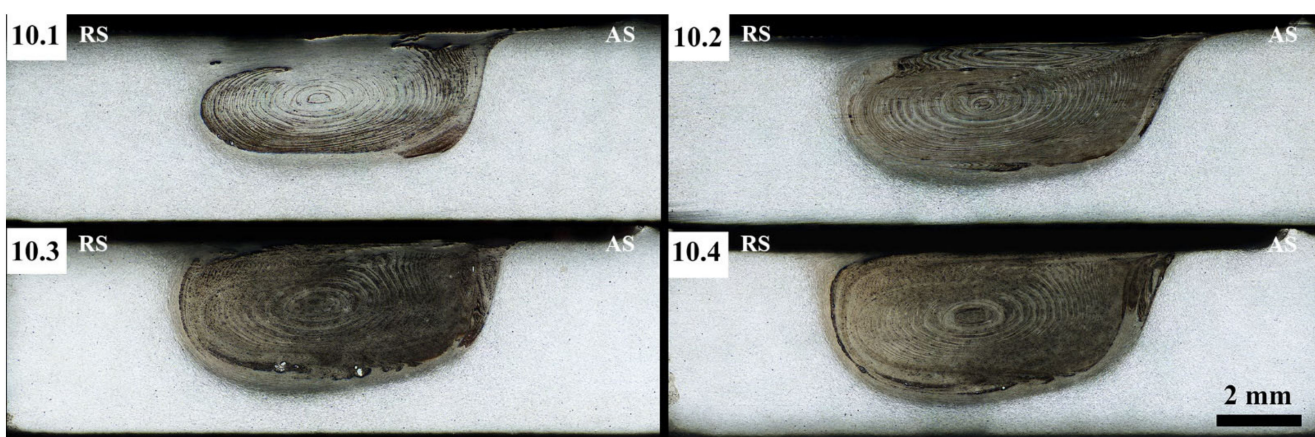


Figure 4. Al-Mg-Sc alloy macrostructure after FSP with 10 wt% Mo after 1–4 passes (samples 10.1–10.4). AS—advancing side, RS—retreating side.

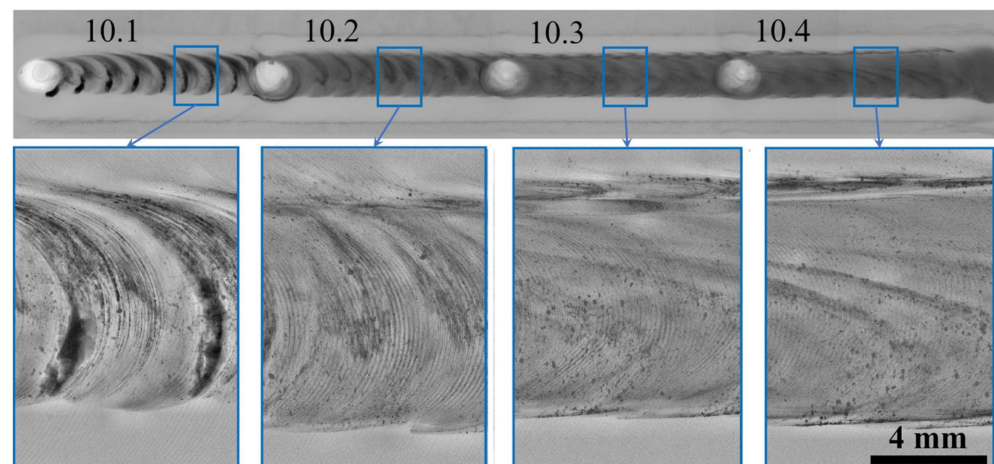


Figure 5. CT images of the processed area of Al-Mg-Sc alloy with 10 wt% Mo.

At 15 wt% Mo after the first pass, the most defective structure is formed in the processed area despite the formation of a single nugget as in the case of 10 wt% Mo (Figure 6 (15.1)). The greatest clusters of powder are observed in the lower nugget part and in the area under the tool shoulders on the advancing side. Moreover, the defectiveness of the stir zone persists even after the second and third passes, as can be seen from the CT data (Figure 7). Figure 6 shows that the defects are predominantly formed in the area under the tool shoulders, and the tomography data show that the process of their formation occurs not only in the areas with holes but also along the entire length of the processed area, predominantly in the stir zone center. The uniform distribution of the alloying element along the length of the processed area without the formation of defects is possible only on the fourth pass, although inside the nugget, the height distribution is relatively uniform already after the second pass, excluding the tool shoulder influence area.

Consequently, one pass is not enough to form a composite based on Al-Mg-Sc alloy and Mo powder, and at least three tool passes are required for the stable distribution of additives in the processed area. The sample with 10 wt% Mo shows the highest stability in the stir zone formation, while the addition of 15 wt% Mo makes the processing most unstable, resulting in many defects even after three passes.

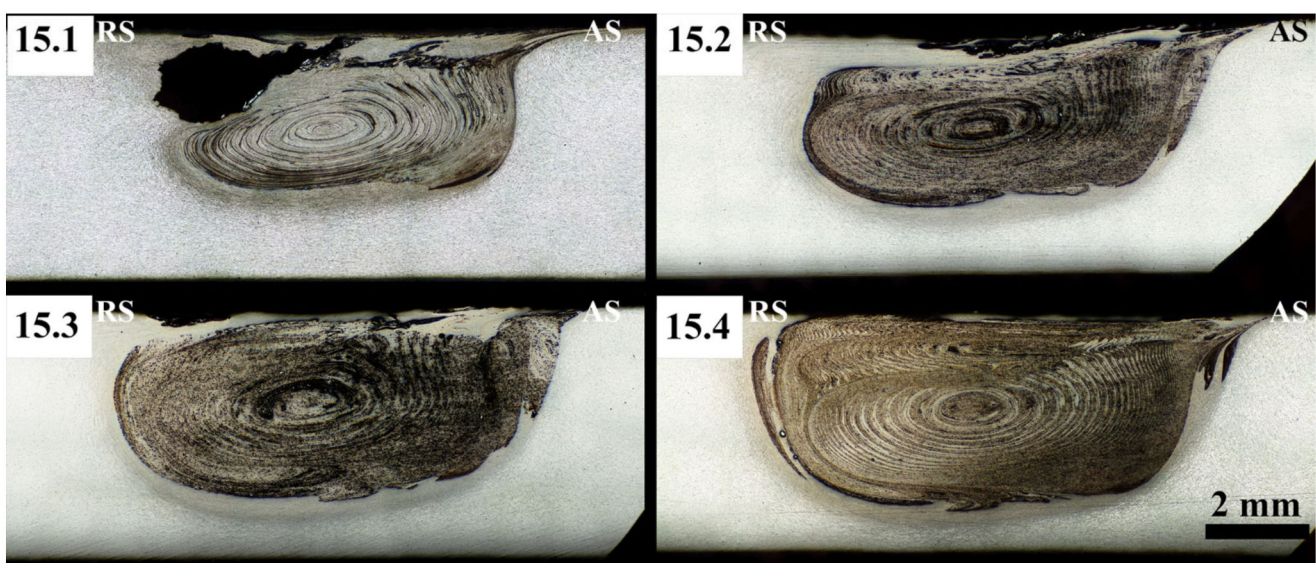


Figure 6. Al-Mg-Sc alloy macrostructure after FSP with 15 wt% Mo after 1–4 passes (samples 15.1–15.4). AS–advancing side, RS–retreating side.

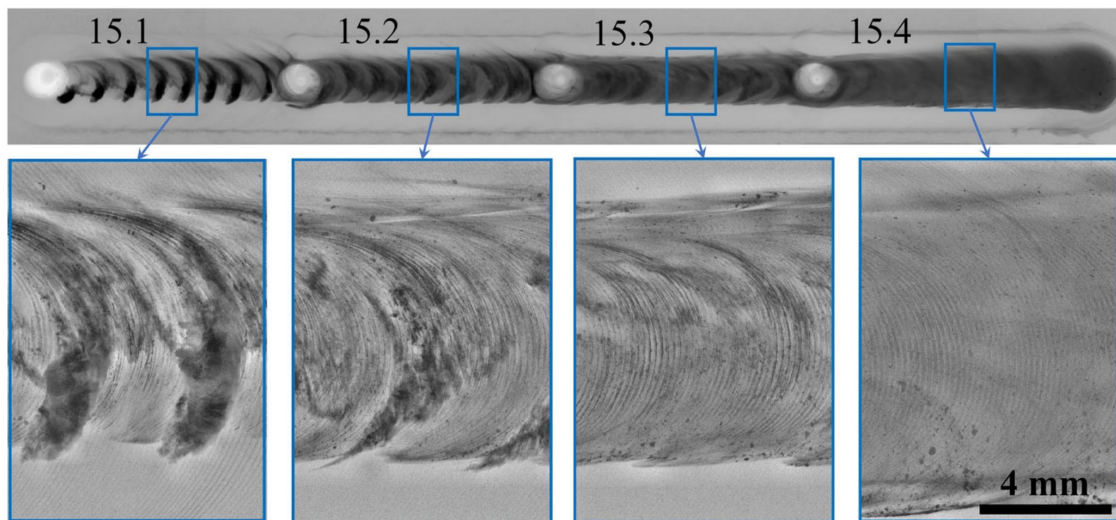


Figure 7. CT images of the processed area of Al-Mg-Sc alloy with 15 wt% Mo.

Nevertheless, in addition to a uniformly formed nugget at the macroscopic level, it is also necessary to understand the interaction of powders with the material to be processed in the stir zone at smaller scale levels. For this purpose, the SZ microstructure was analyzed using transmission electron microscopy techniques.

3.2. Stir Zone Microstructure

The results of transmission electron microscopy (Figure 8) showed that the distribution of Mo particles in the aluminum alloy matrix, even after four passes, is irregular. Both small particles with sizes of tens of nanometers and large clusters of particles with sizes of 0.5 μm and larger can be found. Grain size, in this case, does not differ from the grains of Al-Mg-Sc alloy after friction stir welding without the addition of Mo [23].

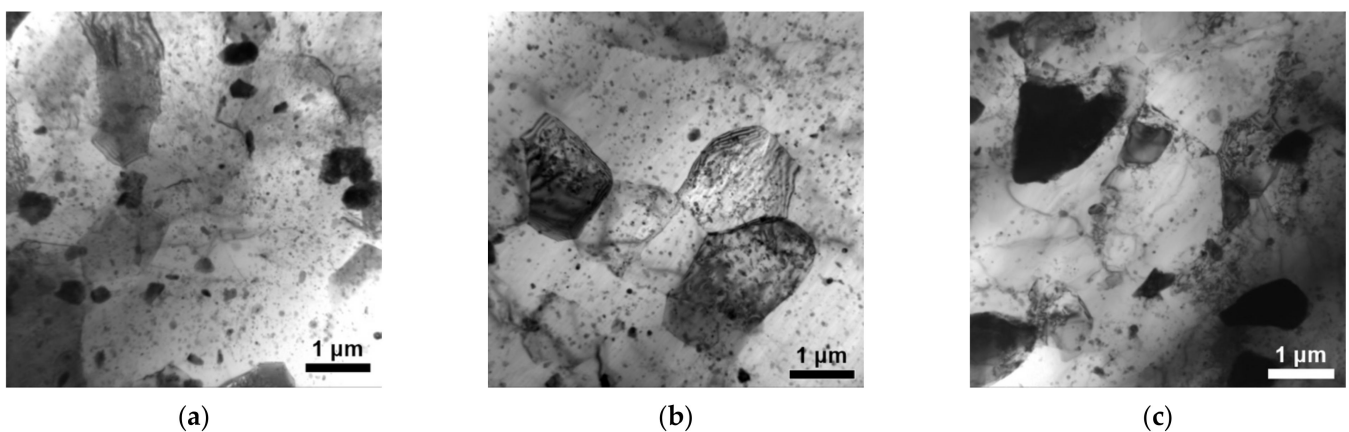


Figure 8. Light-field TEM images of the stir zone of samples (a) 5.4, (b) 10.4 and (c) 15.4.

The STEM analysis showed that even due to multiple severe thermomechanical effects by the FSP method, Mo particles do not interact with the aluminum matrix and alloying elements in any way and do not form intermetallic compounds. Figure 9 shows a STEM image of the stir zone microstructure of an Al-Mg-Sc alloy with Mo inclusions and maps of chemical element distribution in the scanning area in samples 15.1 and 15.4.

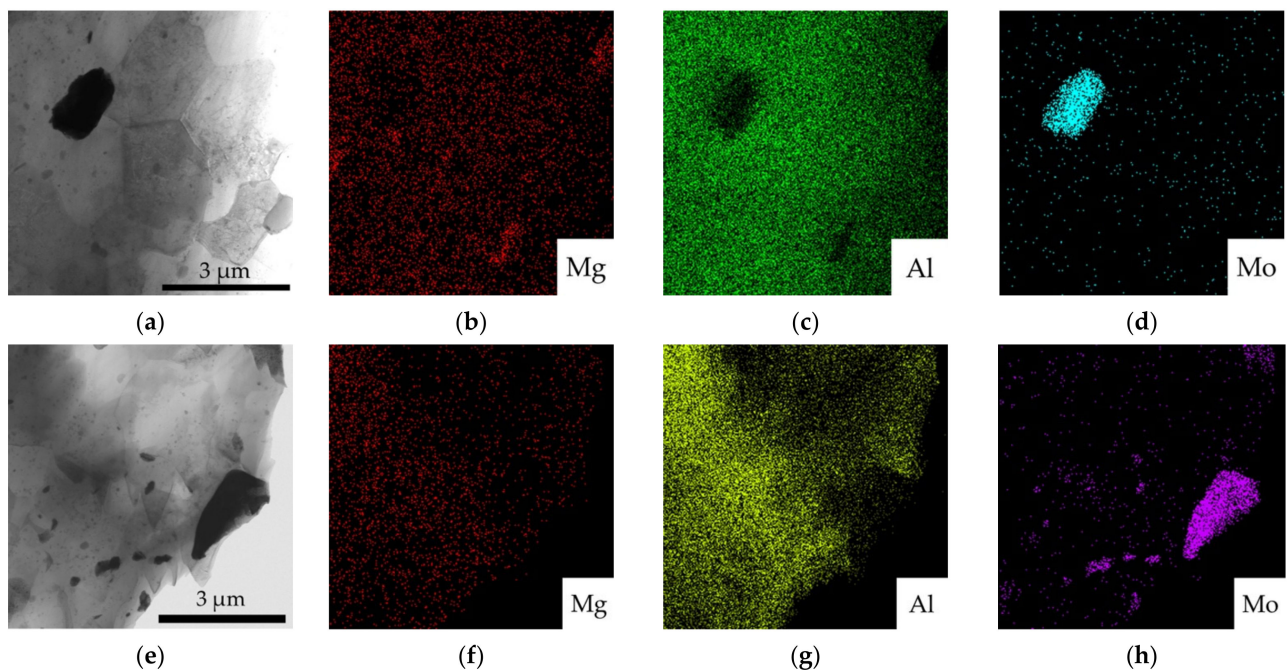


Figure 9. Light-field TEM images of the stir zone and chemical element distribution maps of samples 15.1 (a–d) and 15.4 (e–h).

It should be noted that despite the addition of Mo powder particles, the main grain growth-limiting particles are those of the secondary phase Sc-Al, so grain boundary hardening in the case of Mo alloying is not to be expected. In this regard, it is necessary to study the effect of adding Mo to the alloy on its mechanical characteristics.

3.3. Microhardness

Microhardness measurements in the stir zone showed that the Mo addition leads to a slight increase in microhardness, mainly in the central part of the stir zone. As shown in studies of Al-Mg-Sc alloy welds [23], the microhardness of the base metal is approximately 1.0 GPa, while in the stir zone after FSW, the hardness drops to approximately 0.9 GPa. Measurements of the base metal microhardness of the workpieces used in the present work show that its average values are approximately 0.9 GPa before processing. Figure 10 shows that the addition of 5 wt% Mo in the processing zone at least preserves the properties of the original material in the thermomechanically affected zone and increases values to almost 1.0 GPa near the stir zone center. An increase in the Mo content to 10 wt% and 15 wt% leads to the fact that in the central part of the stir zone, the material microhardness increases up to values of 1.10–1.15 GPa, i.e., an increase of approximately 28% as compared to the base metal.

It is worth noting that the microhardness values were obtained after four passes, and in the case of fewer passes, the distribution of values in the stir zone would be more heterogeneous due to the structural features described in Section 3.1.

3.4. Tensile Properties

The static tensile tests showed that the heterogeneity of Mo distribution in the stir zone and the presence of defects led to a significant decrease in the ductility of the material, as well as a decrease in the tensile strength and yield strength (Figure 11). Thus, samples 5.1 and 5.2, 10.1–10.3, and 15.1–15.3 show insufficient results.

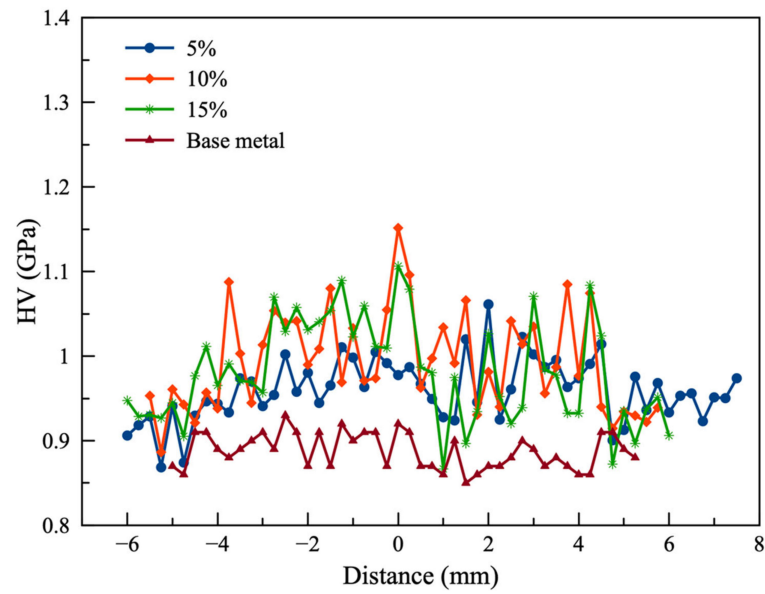


Figure 10. Microhardness profiles of Al-Mg-Sc alloy with Mo addition after four passes.

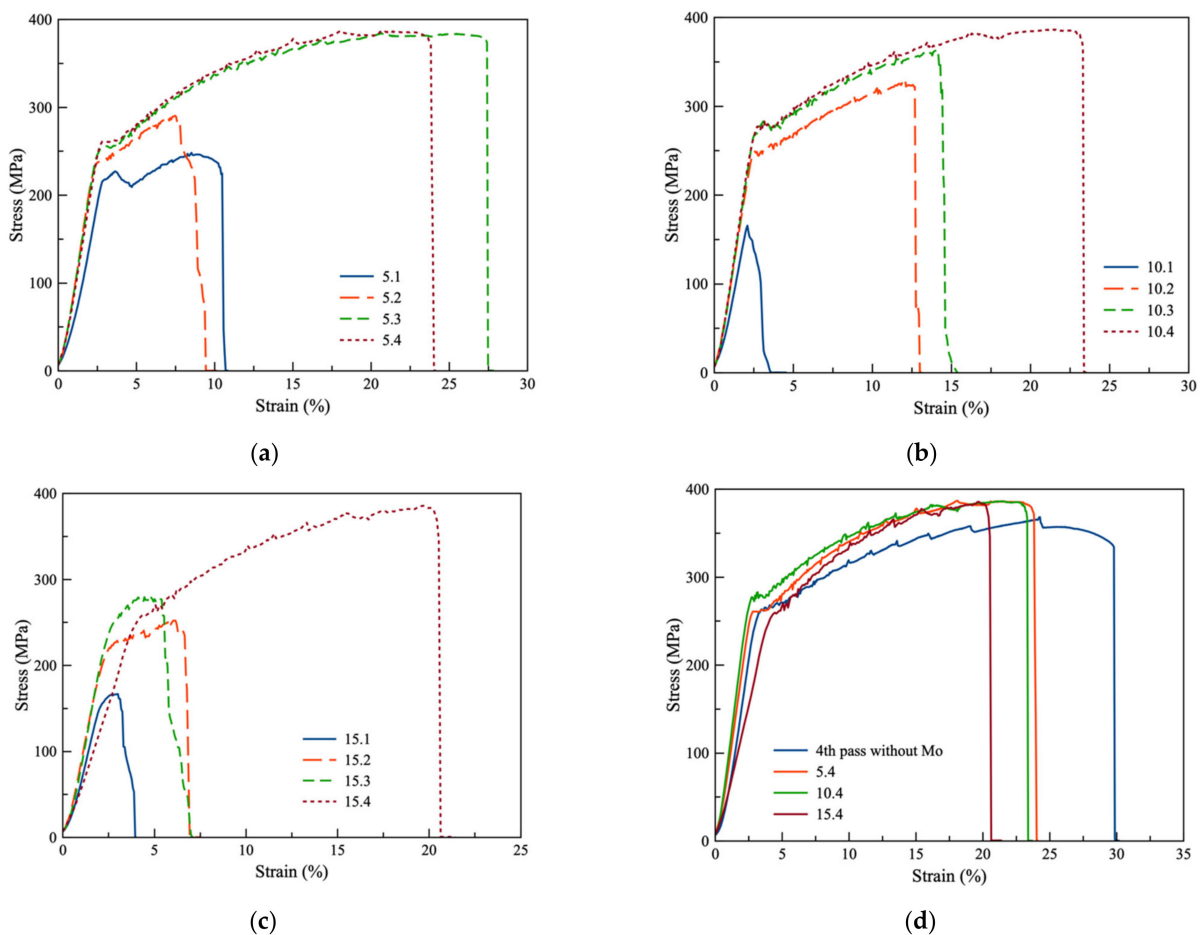


Figure 11. Static tensile test results of samples with 5 wt% Mo (a), 10 wt% Mo (b), and 15 wt% Mo (c), as well as a comparison of the stress–strain curves of the samples after four passes (d).

As can be seen from Figure 11, four tool passes are minimum and sufficient in each case, except for 5 wt% Mo, in which high values of mechanical characteristics are already achieved on the third pass.

When comparing the material properties after four passes (Figure 11d), it can be seen that the ultimate tensile strength of the samples, regardless of the Mo content, is approximately the same (386–387 MPa), and the yield strength is slightly different. Thus, the highest yield strength is observed at 10 wt% Mo (270 MPa), and the lowest—at 15 wt% (250 MPa). As for the material's ductility, the highest results are shown by the sample with 5 wt% Mo, followed by 10 wt% Mo, and 15 wt% Mo again shows the worst result.

3.5. Sliding Wear Al-Mg-Sc/Mo after FSP

In addition to the stable mechanical properties after four tool passes, the Al-Mg-Sc alloy with Mo addition achieves an improvement in the wear resistance of the material in dry sliding friction (Figure 12). However, the effect of Mo is rather controversial. Thus, the sample shows the best result in friction tests with 5 wt% Mo, for which the friction coefficient (CoF) during the test was approximately 0.2. With a further increase in the Mo percentage in the stir zone, the material's wear resistance deteriorates: at 10 wt% Mo, the CoF is at 0.22–0.23, and for 15 wt% Mo is practically equal to the material without Mo—approximately 0.24.

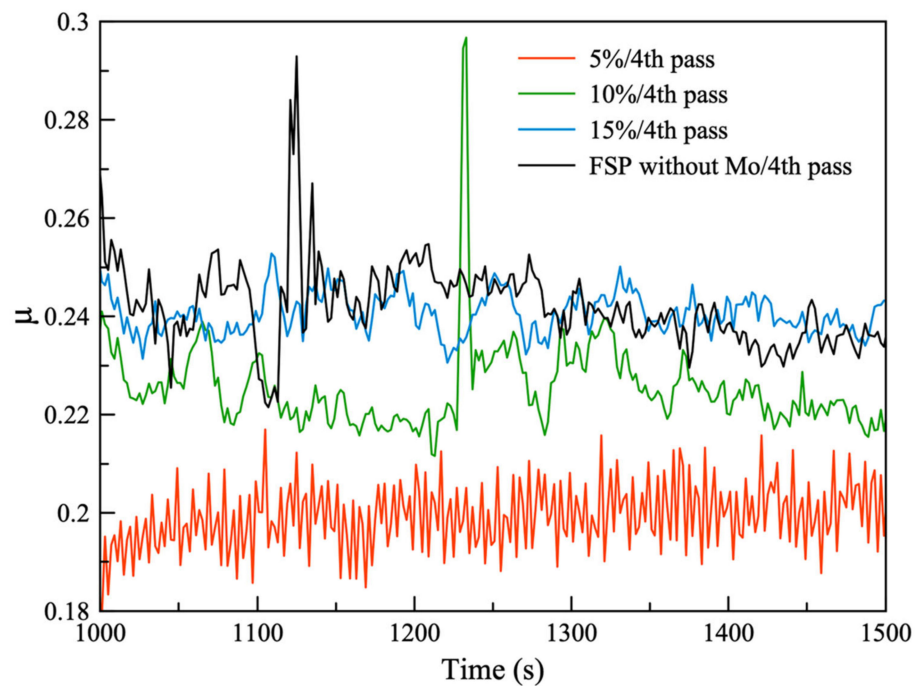


Figure 12. Friction coefficients (μ) of samples after four passes obtained in dry sliding friction tests.

4. Discussion

The results show that producing a composite material based on Al-Mg-Sc alloy and Mo powder using the friction stir processing method is a controversial choice. Firstly, at least four passes are required to evenly distribute the powder in the stir zone (except for the 5 wt% Mo additive, where three passes are sufficient), making the process more time-consuming. For example, the sample with 15 wt% Mo requires four passes to achieve a defect-free stir zone (Figures 6 and 7). Even after three passes, voids are formed in the tool shoulder influence zone, which leads to a drop in the tensile properties of the material, despite a rather uniform distribution of the powder in the SZ main part. This is because in the first stages, the powder is transferred in large clusters, so there is not sufficient material to fill the required volume of the SZ, and this leads to defect formation. Secondly, Mo does not interact with the processed metal even after four tool passes. As a result, no intermetallic compounds are formed in the stir zone. In addition to the fact that no intermetallic compounds are formed at the FSP, the structural analysis results show that Mo is irregularly distributed in the SZ. There is no dependence in the arrangement of

Mo particles in the SZ on the microlevel, and given that the grain size remains similar to the FSW'ed material without Mo, this additive does not affect grain growth. It does not contribute to the material hardening by increasing the grain boundary spreading.

In [7], it was shown that when a composite material based on aluminum alloy and molybdenum powder is produced using electron-beam additive manufacturing, Mo interacts with the aluminum matrix due to high temperatures. As a result, Al_{12}Mo , Al_3Mo_3 , $\text{Al}_{18}\text{Mg}_3\text{Mo}_2$ and other intermetallic compounds are formed when the melt solidifies. However, the microhardness of the material produced in [7] is much lower than in the stir zone of the FSP composite, excluding the areas with intermetallic particles. The stir zone of the Mo-rich Al-Mg-Sc alloy possesses increased microhardness. Samples with high Mo content provide the greatest boost: at 10 wt% and 15 wt% Mo microhardness increases by 28% compared to the base metal. This is because, in the stir zone, the fine-dispersed Mo particles are uniformly distributed to contribute to the increase in microhardness. Nevertheless, even at 5 wt% Mo, the microhardness increases by 10–11% compared to the base metal, in contrast to FSW'ed Al-Mg-Sc alloy, in the SZ of which the microhardness decreases by 10% on average [23].

As for the friction characteristics, the additive material also has no dependence between the Mo content and the CoF: it is lower than that of the original metal only in one case—at 1.2 g powder per layer, whereas at 0.3–0.9 g per layer the CoF is higher or equal to that of the original metal. In our case, the CoF at 15 wt% Mo is approximately equal to the initial metal, and at 5 wt% and 10 wt% Mo is lower, which testifies to the improvement of friction characteristics. Moreover, it can be noted that the less Mo in the stir zone, the lower its CoF. Consequently, a more sophisticated analysis of the effect of Mo content in the Al-Mg-Sc alloy on its friction characteristics will be required in the future, but the data already obtained show that at least 5 wt% Mo in the SZ of the FSP composite allows an increase in the aluminum alloy's strength and wear characteristics. At the same time, despite the absence of hard intermetallic compounds in the SZ, the FSP method of composite production also demonstrates advantages over additive manufacturing, providing improved performance at different Mo concentrations. It is explained by the more homogeneous distribution of fine-dispersed Mo particles due to the stirring process (against additive manufacturing), which provides increased mechanical properties, more uniform microhardness profiles, and better friction characteristics.

Therefore, the data obtained show the effectiveness of the investigated method for producing materials with improved characteristics. However, additional studies are required to determine the optimal concentrations of additives to achieve the maximum effect of structural modification.

5. Conclusions

The following conclusions were drawn as a result of the research conducted:

1. At least three FSW-tool passes are required for the uniform distribution of the Mo powder additive in the stir zone of the Al-Mg-Sc alloy, and the higher the Mo content, the more passes are required. Thus, 10 wt% Mo requires four tool passes, whereas at 15 wt% Mo, after four passes, the material properties are worse than at 10 wt%.
2. The addition of Mo does not influence the process of the dynamic recrystallization of material at FSP. It does not contribute to a reduction in grain size, which remains at the level of the material processed without adding Mo.
3. During the FSP, Mo does not interact with the aluminum alloy matrix, and therefore there is no formation of intermetallic compounds in the stir zone.
4. The stir zone microhardness with Mo powder added after four passes increased by 10–28% compared to the base metal. The higher the Mo content, the higher the microhardness of the processed area.
5. All the samples with Mo added from 5 to 15 wt% after four passes have the same values of the ultimate tensile strength and no considerable difference in the yield

- strength of the material. The material ductility is more noticeably different—23–24 % for 10 and 15 wt% and approximately 15% for 15 wt% Mo.
- The addition of Mo powder influences the friction characteristics of Al-Mg-Sc alloy. Herewith, a positive effect is achieved with a small Mo powder content. Thus, at 5 wt% Mo, the material CoF decreases to 0.2 whereas at 15 wt% Mo, it is equal to 0.24, similar to the Mo-free material. Such a change of friction characteristics requires further investigation of the Mo content effect on the friction coefficient change.

Author Contributions: Conceptualization, T.K., E.K. (Evgeny Knyazhev), and A.C.; methodology, T.K., E.K. (Evgeny Knyazhev), and A.C.; formal analysis, K.K.; investigation, T.K., E.K. (Evgeny Knyazhev), D.G., K.K., N.T., A.V.; validation, T.K., K.K.; resources, A.C.; data curation, T.K. and A.C.; writing—original draft preparation, T.K. and E.K. (Evgeny Knyazhev); writing—review and editing, K.K.; visualization, T.K.; supervision, E.K. (Evgeny Kolubaev); project administration, E.K. (Evgeny Kolubaev); funding acquisition, E.K. (Evgeny Kolubaev). All authors have read and agreed to the published version of the manuscript.

Funding: The work was performed according to the Government research assignment for ISPMS SB RAS, project FWRW-2021-0012.

Institutional Review Board Statement: Not applicable.

Informed Consent Statement: Not applicable.

Data Availability Statement: Not applicable.

Conflicts of Interest: The authors declare no conflict of interest.

References

- Rafieezad, M.; Mohammadi, M.; Gerlich, A.; Nasiri, A. Enhancing the corrosion properties of additively manufactured AlSi10Mg using friction stir processing. *Corros. Sci.* **2021**, *178*, 109073. [[CrossRef](#)]
- Kalashnikova, T.; Chumaevsii, A.; Kalashnikov, K.; Knyazhev, E.; Gurianov, D.; Panfilov, A.; Nikonov, S.; Rubtsov, V.; Kolubaev, E. Regularities of Friction Stir Processing Hardening of Aluminum Alloy Products Made by Wire-Feed Electron Beam Additive Manufacturing. *Metals* **2022**, *12*, 183. [[CrossRef](#)]
- Yang, T.; Wang, K.; Wang, W.; Peng, P.; Huang, L.; Qiao, K.; Jin, Y. Effect of Friction Stir Processing on Microstructure and Mechanical Properties of AlSi10Mg Aluminum Alloy Produced by Selective Laser Melting. *J. Miner. Met. Mater. Soc.* **2019**, *71*, 1737–1747. [[CrossRef](#)]
- Georgantzia, E.; Gkantou, M.; Kamaris, G.S. Aluminium alloys as structural material: A review of research. *Eng. Struct.* **2021**, *227*, 111372. [[CrossRef](#)]
- Pramanik, A. Effects of Reinforcement on Wear Resistance of Aluminum Matrix Composites. *Trans. Nonferrous Met. Soc. China* **2016**, *26*, 348–358. [[CrossRef](#)]
- Rajmohan, T.; Palanikumar, K.; Ranganathan, S. Evaluation of Mechanical and Wear Properties of Hybrid Aluminium Matrix Composites. *Trans. Nonferrous Met. Soc. China* **2013**, *23*, 2509–2517. [[CrossRef](#)]
- Zykova, A.; Chumaevsii, A.; Vorontsov, A.; Shamarin, N.; Panfilov, A.; Knyazhev, E.; Moskvichev, E.; Gurianov, D.; Savchenko, N.; Kolubaev, E.; et al. Microstructural Evolution of AA5154 Layers Intermixed with Mo Powder during Electron Beam Wire-Feed Additive Manufacturing (EBAM). *Metals* **2022**, *12*, 109. [[CrossRef](#)]
- Boopathi, S.; Jeyakumar, M.; Singh, G.R.; King, F.L.; Pandian, M.; Subbiah, R.; Haribalaji, V. An Experimental Study on Friction Stir Processing of Aluminium Alloy (AA-2024) and Boron Nitride (BNp) Surface Composite. *Mater. Today Proc.* **2022**, *59*, 1094–1099. [[CrossRef](#)]
- Ikumapayi, O.M.; Akinlabi, E.T.; Abegunde, O.O.; Fayomi, O.S.I. Electrochemical Investigation of Calcined Agrowastes Powders on Friction Stir Processing of Aluminium-Based Matrix Composites. *Mater. Today Proc.* **2020**, *26*, 3238–3245. [[CrossRef](#)]
- Khosshaim, A.B.; Moustafa, E.B.; Bafakeeh, O.T.; Elsheikh, A.H. An Optimized Multilayer Perceptrons Model Using Grey Wolf Optimizer to Predict Mechanical and Microstructural Properties of Friction Stir Processed Aluminum Alloy Reinforced by Nanoparticles. *Coatings* **2021**, *11*, 1476. [[CrossRef](#)]
- Khodabakhshi, F.; Simchi, A.; Kokabi, A.H.; Gerlich, A.P. Friction Stir Processing of an Aluminum-Magnesium Alloy with Pre-Placing Elemental Titanium Powder: In-Situ Formation of an Al3Ti-Reinforced Nanocomposite and Materials Characterization. *Mater. Charact.* **2015**, *108*, 102–114. [[CrossRef](#)]
- Asrari, G.; Daneshifar, M.H.; Hosseini, S.A.; Alishahi, M. Fabrication of Al-Mg Solid Solution by Friction Stir Selective Alloying. *Mater. Lett.* **2022**, *308*, 131073. [[CrossRef](#)]
- Mohan, V.K.; Shammadh, M.; Sudheer, A. Fabrication and Characterization of Friction Stir Welding of AA6061 Using Copper Powder. *Mater. Today Proc.* **2018**, *5*, 24339–24346. [[CrossRef](#)]

14. Balakrishnan, M.; Dinaharan, I.; Kalaiselvan, K.; Palanivel, R. Friction Stir Processing of Al3Ni Intermetallic Particulate Reinforced Cast Aluminum Matrix Composites: Microstructure and Tensile Properties. *J. Mater. Res. Technol.* **2020**, *9*, 4356–4367. [[CrossRef](#)]
15. Izadi, H.; Nolting, A.; Munro, C.; Bishop, D.P.; Plucknett, K.P.; Gerlich, A.P. Friction Stir Processing of Al/SiC Composites Fabricated by Powder Metallurgy. *J. Mater. Process. Technol.* **2013**, *213*, 1900–1907. [[CrossRef](#)]
16. Mishra, R.S.; Ma, Z.Y.; Charit, I. Friction Stir Processing: A Novel Technique for Fabrication of Surface Composite. *Mater. Sci. Eng. A* **2003**, *341*, 307–310. [[CrossRef](#)]
17. Kumar Patel, S.; Pratap Singh, V.; Kumar, D.; Saha Roy, B.; Kuriachen, B. Microstructural, Mechanical and Wear Behavior of A7075 Surface Composite Reinforced with WC Nanoparticle through Friction Stir Processing. *Mater. Sci. Eng. B* **2022**, *276*, 115476. [[CrossRef](#)]
18. Patel, S.K.; Singh, V.P.; Roy, B.S.; Kuriachen, B. Microstructural, Mechanical and Wear Behavior of A7075 Surface Composite Reinforced with WC and ZrSiO₄ Nanoparticle through Friction Stir Processing. *J. Manuf. Process.* **2021**, *71*, 85–105. [[CrossRef](#)]
19. Yang, X.; Zhang, H.; Dong, P.; Yan, Z.; Wang, W. A Study on the Formation of Multiple Intermetallic Compounds of Friction Stir Processed High Entropy Alloy Particles Reinforced Al Matrix Composites. *Mater. Charact.* **2022**, *183*, 111646. [[CrossRef](#)]
20. Shehabeldeen, T.A.; El-Shafai, N.M.; El-Mehasseb, I.M.; Yin, Y.; Ji, X.; Shen, X.; Zhou, J. Improvement of Microstructure and Mechanical Properties of Dissimilar Friction Stir Welded Aluminum/Titanium Joints via Aluminum Oxide Nanopowder. *Vacuum* **2021**, *188*, 110216. [[CrossRef](#)]
21. Lee, I.S.; Kao, P.W.; Chang, C.P.; Ho, N.J. Formation of Al–Mo Intermetallic Particle-Strengthened Aluminum Alloys by Friction Stir Processing. *Intermetallics* **2013**, *35*, 9–14. [[CrossRef](#)]
22. Selvakumar, S.; Dinaharan, I.; Palanivel, R.; Ganesh Babu, B. Characterization of Molybdenum Particles Reinforced Al6082 Aluminum Matrix Composites with Improved Ductility Produced Using Friction Stir Processing. *Mater. Charact.* **2017**, *125*, 13–22. [[CrossRef](#)]
23. Kalashnikova, T.; Chumaeveskii, A.; Kalashnikov, K.; Fortuna, S.; Kolubaev, E.; Tarasov, S. Microstructural Analysis of Friction Stir Butt Welded Al-Mg-Sc-Zr Alloy Heavy Gauge Sheets. *Metals* **2020**, *10*, 806. [[CrossRef](#)]